JB Journals.ASM.org

Cluster of Genes That Encode Positive and Negative Elements Influencing Filament Length in a Heterocyst-Forming Cyanobacterium

Victoria Merino-Puerto,* Antonia Herrero, Enrique Flores

Instituto de Bioquímica Vegetal y Fotosíntesis, Consejo Superior de Investigaciones Científicas and Universidad de Sevilla, Seville, Spain

The filamentous, heterocyst-forming cyanobacteria perform oxygenic photosynthesis in vegetative cells and nitrogen fixation in heterocysts, and their filaments can be hundreds of cells long. In the model heterocyst-forming cyanobacterium *Anabaena* sp. strain PCC 7120, the genes in the *fraC-fraD-fraE* operon are required for filament integrity mainly under conditions of nitrogen deprivation. The *fraC* operon transcript partially overlaps gene *all2395*, which lies in the opposite DNA strand and ends 1 bp beyond *fraE*. Gene *all2395* produces transcripts of 1.35 kb (major transcript) and 2.2 kb (minor transcript) that overlap *fraE* and whose expression is dependent on the N-control transcription factor NtcA. Insertion of a gene cassette containing transcriptional terminators between *fraE* and *all2395* prevented production of the antisense RNAs and resulted in an increased length of the cyanobacterial filaments. Deletion of *all2395* resulted in a larger increase of filament length and in impaired growth, mainly under N_2-fixing conditions and specifically on solid medium. We denote *all2395* the *fraF* gene, which encodes a protein restricting filament length. A FraF-green fluorescent protein (GFP) fusion protein accumulated significantly in heterocysts. Similar to some heterocyst differentiation-related proteins such as HglK, HetL, and PatL, FraF is a pentapeptide repeat protein. We conclude that the *fraC-fraD-fraE*←*fraF* gene cluster (where the arrow indicates a change in orientation), in which *cis* antisense RNAs are produced, regulates morphology by encoding proteins that influence positively (FraC, FraD, FraE) or negatively (FraF) the length of the filament mainly under conditions of nitrogen deprivation. This gene cluster is often conserved in heterocyst-forming cyanobacteria.

Bacteria are commonly considered unicellular organisms, but some multicellular bacteria do exist. There are bacteria that grow as filaments of cells, and examples of this include *Streptomyces* (1), *Chloroflexus* (2), the recently described filamentous *Desulfobulbaceae* (3), and some cyanobacterial species (4). Many cyanobacteria form trichomes (filaments of cells), some of which exhibit cellular differentiation processes. When incubated in the absence of a source of combined nitrogen, filaments of some cyanobacteria present two cell types: vegetative cells that perform oxygenic photosynthesis and heterocysts that perform N_2 fixation (4). In *Anabaena* and *Nostoc*, heterocysts are spaced along the filament and differentiate from vegetative cells in a process that involves execution of a specific program of gene expression (5–7). Two positive-acting regulators are required for the initiation of heterocyst differentiation: NtcA, which is the global nitrogen control transcription factor of cyanobacteria, and HetR, which is a differentiation-specific factor (4, 5, 7). NtcA is known to bind to DNA sites with the consensus sequence GTA-N_8-TAC (8), of which GT-N_{10}-AC is an important subset (9). In the N_2-fixing filament, the heterocysts provide the vegetative cells with fixed nitrogen and the vegetative cells provide the heterocysts with photosynthate (7). Thus, being multicellular in nature is essential for heterocyst-forming cyanobacteria to grow. The cyanobacteria are diderm bacteria (10), carrying an outer membrane outside the cytoplasmic membrane and the peptidoglycan layer (11). In filamentous cyanobacteria, whereas the cytoplasmic membrane and peptidoglycan layer surround each cell, the outer membrane is continuous along the filament, defining a continuous periplasm (12–15).

Regulatory RNAs influencing gene expression have been amply documented in bacteria (16). They can be small RNAs that are encoded at a distance from the target gene and therefore act in *trans* (17) or genuine antisense RNAs that are transcribed from the DNA strand opposite the sense strand of the target gene and therefore act in *cis* (18, 19). In cyanobacteria, a plethora of potential regulatory small RNAs have been identified (20, 21), and genuine antisense RNAs are also being found. An example of the latter is found in the *furA* genomic region of the cyanobacterium *Anabaena* sp. strain PCC 7120 (22). The transcript of the *furA* downstream gene, *alr1690*, which lies in the opposite DNA strand, extends as an antisense RNA covering the whole *furA* gene and influences production of the FurA protein (22).

In the model heterocyst-forming cyanobacterium *Anabaena* sp. strain PCC 7120, genes whose mutation results in filament fragmentation and some of which encode cell-cell-joining proteins are known (23–29). The *fraC* operon comprises three genes, *fraC*, *fraD*, and *fraE*, which are required for *Anabaena* to make long filaments mainly under diazotrophic conditions (28, 30). FraC, FraD, and FraE are integral membrane proteins, and at least FraC and FraD are located at the intercellular septa in the *Anabaena* filament. FraC and FraD may together constitute a septal protein complex that joins the adjacent cells and mediates intercellular molecular exchange (30). These genes are expressed in a 3.1-to-3.3-kb, low-abundance transcript that is not responsive to the nitrogen source (28). In this work, we show the presence of a nitrogen-regulated *fraE* antisense RNA that is an extension of the

Received 14 February 2013 **Accepted** 21 June 2013

Published ahead of print 28 June 2013

Address correspondence to Enrique Flores, eflores@ibvf.csic.es.

* Present address: Victoria Merino-Puerto, Departamento de Genética, Facultad de Biología, Universidad de Sevilla, Seville, Spain.

doi:10.1128/JB.00181-13

transcript of *all2395*, a gene that resides in the opposite DNA strand in a tail-to-tail arrangement to *fraE* and that we denote *fraF*. The *fraCDE* transcript also extends as an antisense RNA into *fraF*. We have observed a moderate effect of disruption of the *cis* antisense RNAs and a larger effect of deletion of *fraF*, a gene that influences negatively the length of the *Anabaena* filaments.

MATERIALS AND METHODS

Strains and growth conditions. *Anabaena* sp. (also known as *Nostoc* sp.) strain PCC 7120 was grown at 30°C in the light (25 μmol m^{-2} s^{-1}) in shaken (100 rpm) liquid cultures or in medium solidified with 1% Difco agar. The medium used was BG11 (which contains $NaNO_3$ as the nitrogen source [31]) modified to contain ferric citrate instead of ferric ammonium citrate; $BG11_0$ (BG11 further modified by omission of $NaNO_3$); or $BG11_0$ plus ammonium [$BG11_0$ containing 4 mM NH_4Cl and 8 mM *N*-tris(hydroxymethyl)methyl-2-aminoethanesulfonic acid (TES)–NaOH buffer, pH 7.5]. Alternatively, cultures (referred to as bubbled cultures and denoted BG11C or $BG11_0C$) were supplemented with 10 mM $NaHCO_3$ and bubbled with a mixture of air and 1% (vol/vol) CO_2 in the light (50 to 75 μmol m^{-2} s^{-1}). In this case, the ammonium-containing medium was supplemented with 6 mM NH_4Cl and 12 mM TES-NaOH buffer (pH 7.5). For the mutants described below, the following antibiotics (concentrations) were used: in liquid cultures, streptomycin sulfate (Sm) (2 to 5 μg ml^{-1}), spectinomycin dihydrochloride pentahydrate (Sp) (2 to 5 μg ml^{-1}), and neomycin sulfate (Nm) (10 to 20 μg ml^{-1}); and in solid media, Sm (5 μg ml^{-1}), Sp (5 μg ml^{-1}), and Nm (40 μg ml^{-1}). *Escherichia coli* DH5α, used for plasmid constructions, and other strains of *E. coli* (see below) were grown in LB medium, supplemented when appropriate with antibiotics at standard concentrations (32).

Strain constructions. DNA was isolated from *Anabaena* sp. by the method of Cai and Wolk (33). To remove an internal fragment from *all2395*, a 646-bp DNA fragment from the 3′ region of *all2395* and part of *alr2394* was amplified by PCR with oligodeoxynucleotide primers alr2394-1 (which contains a BamHI restriction site in its 5′ end) and all2395-8, and a 602-bp fragment from *all2395* 5′ and upstream sequences was amplified with primers all2395-5 and all2395-10 (which contains a BamHI restriction site in its 5′ end). (All oligodeoxynucleotide primers are shown in Table 1.) The amplified fragments were joined together by the megaprimer PCR protocol (32), cloned into vector pMBL-T (Dominion MBL, Spain), and transferred to BamHI-digested pCSRO, producing pCSVT60, which carries a cloned *Anabaena* DNA fragment with a 594-bp deletion of *all2395*. (Plasmid pCSRO is a fusion of a 3,193-bp DraI fragment bearing *bom*, *oriV*, and an *rpoA*-interrupted polylinker from pCSV3 [34] and a 4,250-bp EcoRV fragment bearing an Sm^r Sp^r determinant and the *sacB* gene for positive selection from pRL277 [35].)

To insert the Sm^r Sp^r C.S3 gene cassette (36) between open reading frames (ORFs) *alr2394* and *all2395*, a 806-bp DNA fragment that included *alr2394* was amplified by PCR with primers alr2394-5 and alr2394-8 (which contains an EcoRV restriction site close to its 5′ end), and a 924-bp DNA fragment that included *all2395* was amplified with primers all2395-3 (which contains an EcoRV restriction site close to its 5′ end) and all2395-6. The amplified fragments were joined together by the megaprimer PCR protocol (32) and cloned into vector pMBL-T, producing pCSVT64. The C.S3 cassette, removed from pCSV3 (34) by DraI digestion, was cloned into EcoRV-digested pCSVT64, and the whole *alr2394-C.S3-all2395* construct was transferred as a NheI-SpeI fragment to XbaI-digested pRL278 (*sacB*, Nm^r Km^r [35]), producing pCSVT65.

Conjugation of *Anabaena* sp. strain PCC 7120 with *E. coli* HB101 carrying pCSVT60 or pCSVT65 with helper and methylation plasmid pRL623 was effected by the use of the conjugative plasmid pRL443, carried in *E. coli* ED8654, and performed as described previously (37) with selection for resistance to Sm-Sp (pCSVT60) or Sm-Sp and Nm (pCSVT65). Exconjugants carrying only chromosomes with the inserted plasmids were then used to isolate double-recombinant clones resistant to 5% sucrose (33). The genetic structure of selected clones was studied by PCR with DNA from those clones and primer pair alr2394-3 and all2396-2 for strain CSVT24 and primer pair C.S3-2 and all2396-2 and primer pair alr2393-25 and all2396-2 for strain CSVT25. Strain CSVT24 contained only mutant chromosomes with the internal deletion of *all2395* and, because the mutation was unmarked, was grown without antibiotic selection. Strain CSVT25 contained only chromosomes carrying the insertion of C.S3 between *alr2394* and *all2395* and was grown in the presence of Sm and Sp.

For construction of an All2395-green fluorescent protein (GFP) fusion, two DNA fragments were amplified by PCR using *Anabaena* DNA as the template and cloned into vector pSpark (Canvax). (i) A 798-bp fragment carrying the *alr2394* sequence was amplified with primers alr2394-9 (which contains an EcoRI restriction site in its 5′ end) and alr2394-12 (which contains a SmaI restriction site in its 5′ end). (ii) A 909-bp fragment carrying *all2395* and a short upstream sequence was amplified with primers all2395-15 [which contains in its 5′ end an NheI restriction site that removes the stop codon of the gene and a series of nucleotides whose inverted sequence provides a $(Gly)_4$ sequence] and all2395-16 (which contains a HindIII restriction site in its 5′ end). The *all2395* gene was transferred as an NheI-HindIII fragment to NheI-HindIII-digested pCSAL34 (which contains, cloned in vector pMBL-T, the gene encoding a superfolder [sf]-GFP with an Ala-encoding codon instead of the Met start codon), producing pCSVT81. The *alr2394* gene was transferred as an EcoRI-SmaI fragment to EcoRI-SmaI-digested pCSVT81, producing pCSVT83. The whole *alr2394-sf.gfp-all2395* construct (note that *sf.gfp* is fused to the 3′ end of *all2395*) was transferred as a PstI-BamHI fragment to PstI-BglII-digested pRL277 (*sacB*, Sm^r Sp^r [35]), producing pCSVT84.

TABLE 1 Oligodeoxynucleotide primers used in this work

Primer	Sequence (5′ → 3′)[a]
fraC-4	GAT ATC CTG CGG TTC TTC TTG
fraC-7	GGA TCC TTC ACC TTA AGT GAA GAT ATA GG
fraC-12	CTT GCT TTC GCC TAC CTA TTA
alr2393-1	TAT AGG GAA AAA GCA AGA AGA A
alr2393-5	AAT GCG ATC GCT TGA ATA
alr2393-7	GAT GAC CCC TTA AGA GTT CCT
alr2393-13	GGA TCC ACA CTG ACT CTA AAC TCG G
alr2393-25	TGT TGA ACC GCG TGT AGT C
alr2394-1	CGG ATC CGT GGC GAT GAG
alr2394-2	GGA TCC CGG CTA AAC TCT ACT AT
alr2394-3	ATC GAT ATT ATC GCT GTC TTT GTG
alr2394-5	GGG TAA TGG GGA GAA TGA CT
alr2394-8	AAT GAT GAT ATC TTA AAA CTC CCG GCG TGA A
alr2394-9	GAA TTC GGG AGA ATG ACT ATG ATG AGA
alr2394-12	CCC GGG TTT AAA ACT CCC GGC GTG
all2395-3	TTT TAA GAT ATC ATC ATT CCC AAA TCA CTA T
all2395-4	GGA TCC GTA ATT TGA GTG
all2395-5	ATT GCA CAG GAG TAA TGC TTG TGG T
all2395-6	ATC AAT TCC CCA TCA CCT T
all2395-7	AAT TGC GAT CGC CAT AAC AA
all2395-8	CTC CTG TGC AAT CCC CAA ATA GTG
all2395-9	CACCACTTAAATCAACTGTA
all2395-10	GGA TCC ATT AAA GGC TAC GG
all2395-12	AGG GCA ATT TAT CCA GAG C
all2395-13	TCA GGC ATA ATG GTA TCG C
all2395-15	GCT AGC **ACC GCC TCC ACC** TTC CCA AAT CAC TAT T
all2395-16	AAG CTT CTC GTC ATC AAT TCC CCA TCA
all2396-2	AGG CGG AGC ATT TTT ACC
C.S3-2	GTT ACC CGA GAG CTT GGC
gfp-4	CAA GAA TTG GGA CAA CTC C
rnpB-4	ACT CTT GGT AAG GGT GCA AAG GTG
rnpB-5	AAC CAT AGT TCC TTC GGC CTT GCT

[a] Introduced restriction enzyme cutting sites are underlined. Introduced Gly-encoding codons are shown in bold.

This plasmid was transferred to *Anabaena* sp. strain PCC 7120 by conjugation as described above. Sm^r Sp^r clones that should have had incorporated into their genome the whole pCSVT84 by a single recombination event were selected. Then, clones resistant to 5% sucrose were isolated and tested for sensitivity to Sm and Sp. Sucrose^r Sm^s Sp^s clones should have lost the vector portion of pCSVT84 through a second recombination event. Strain CSVT29 contained only chromosomes carrying the *all2395-sf.gfp* fusion gene as corroborated by PCR with primers alr2393-25 and all2396-2 (both lying outside the construct) and all2396-2 and gfp-4.

Northern blot, primer extension, reverse transcription-PCR (RT-PCR), and quantitative RT-PCR (Q-RT-PCR) analyses. Total RNA was isolated from *Anabaena* sp. as described previously for Gram-negative bacteria (32). For Northern blots, 15 μg of RNA was loaded per lane and electrophoresed in denaturing 1% agarose formaldehyde gels. Hybridizations were performed as previously described (38). Double-stranded DNA probes were generated by PCR using *Anabaena* DNA as the template and the oligonucleotide primers indicated in each case, and they were labeled with a DNA labeling kit (Ready to Go; Amersham Pharmacia Biotech) and [α-^{32}P]dCTP. Single-stranded probes were generated by PCR with the indicated primer and a double-stranded probe (previously generated by conventional PCR) as the template, and they were labeled by inclusion of [α-^{32}P]dCTP in the PCR. As a control of RNA loading and transfer efficiency, the filters were hybridized with a probe of the RNase P RNA gene (*rnpB*) from strain PCC 7120 (39).

For primer extension, 25 μg of RNA isolated from the indicated cultures was used with primers that were labeled with polynucleotide kinase and [γ-^{32}P]dATP. The primers used were all2395-7 and all2395-9. The extension reactions were performed and the gels were run as previously described (40). Radioactive areas in Northern blot hybridizations and primer extension analysis were visualized and quantified with a Cyclone storage phosphor system (Packard).

For RT-PCR, 10 μg of strain PCC 7120 total RNA was mixed with 40 pmol of oligonucleotide (alr2393-5, alr2393-7, or alr2393-13) in the presence of 10 mM Tris-HCl [pH 8.0], 150 mM KCl, and 1 mM EDTA and heated for 10 min at 85°C and then at 50°C for 1 h for annealing. The extension reactions were carried out at 47°C for 1 h in a final volume of 45 μl containing the whole annealing reaction mixture, 0.25 mM (each) deoxynucleoside triphosphates, 200 U of reverse transcriptase (Superscript II; Invitrogen), and the buffer recommended by the transcriptase provider. To control for the presence of contaminating DNA, samples containing 10 μg of RNA, 40 pmol of oligonucleotides, and 1 μg of RNase A (DNase free; Roche) were incubated in a 45-μl reaction volume at 37°C for 15 min. PCR was carried out with 2 to 5 μl of retrotranscription mixture or RNase-treated sample as the template and oligonucleotide pair alr2393-5 and all2595-12, oligonucleotide pair alr2393-7 and all2595-12, or oligonucleotide pair alr2393-13 and all2595-12 as primers. Samples containing the same oligonucleotides and strain PCC 7120 genomic DNA as the template were run in parallel and used as a control. PCR was performed by standard procedures, and the PCR products were resolved by electrophoresis in a 0.7% agarose gel.

For Q-RT-PCR of *fraC* transcripts, total RNA was isolated from cultures of strains PCC 7120, CSVT24, and CSVT25 incubated without combined nitrogen for 0, 6, and 9 h. For elimination of genomic DNA and retrotranscription, 1 μg of RNA was treated with a Quantitect Reverse transcription kit (Qiagen) following the instructions from the supplier. An RT control reaction mixture, in which the RT enzyme was absent, was always included to rule out amplification of contaminant DNA. cDNA was amplified by PCR with two primer pairs corresponding to *fraC*, primer pair alr2393-1 and fraC-12 and primer pair fraC-7 and fraC-4 and with a primer pair corresponding to *rnpB*, rnpB-4 and rnpB-5, that was used as a control (Table 1). The thermal cycling program consisted of an initial preheating step of 10 s at 95°C followed by 40 cycles of 5 s at 95°C and 20 s at 60°C and a dissociation step of 1 s at 95°C. The generation of products was monitored after each extension step by measuring the fluorescence intensity of double-stranded DNA binding SYBR green I dye (TaKaRa) using a Roche LightCycler 480 II instrument. The cycle threshold (C_T) value was determined for each gene and RNA sample in triplicate, and the relative values of expression were derived from the corresponding 2^{-CT} values using the *rnpB* gene as a reference.

Growth rates and microscopy. The growth rate constant ($\mu = \ln 2/t_d$, where t_d is the doubling time) was calculated from the increase of protein content, determined in 0.2-ml samples, of shaken liquid cultures (41). Protein concentration was determined by a modified Lowry procedure (42). Chlorophyll *a* (Chl) content of cultures was determined by the method of Mackinney (43).

For standard light microscopy, filaments grown in BG11 or BG11$_0$ medium plus ammonium (in the presence of Sm and Sp for the CSVT25 mutant) with shaking were harvested, washed with nitrogen-free medium, resuspended in BG11$_0$ medium, and incubated for the indicated times at 30°C in the light on a shaker. Samples taken with great care to prevent disruption were visualized by standard light microscopy. For determining filament sizes (number of cells per filament), 150 to 300 filaments were counted from each culture or cell suspension. Comparison of the distributions of filament sizes of different strains under different culture conditions was assessed by the χ^2 test.

GFP fluorescence was analyzed by confocal microscopy. Samples from cultures of *Anabaena* sp. set atop solidified medium were visualized using a Leica HCX PLAN-APO 63× 1.4 numerical aperture (NA) oil immersion objective attached to a Leica TCS SP2 confocal laser scanning microscope. GFP was excited using 488-nm irradiation from an argon ion laser, and fluorescent emission was monitored from 500 to 538 nm. Under the conditions used, optical section thickness was about 0.4 μm. GFP fluorescence intensity was analyzed using ImageJ 1.43m software.

RESULTS

***fraE* antisense RNA.** As mentioned above, the *fraC* operon (Fig. 1A) is expressed as a 3.1-to-3.3-kb low-abundance transcript (28). Northern blot analysis carried out with a double-stranded probe of the *fraE* gene (probe 1) showed, however, a transcript of higher abundance that was about 1.35 kb in size (Fig. 1B). Because this transcript could not be observed with a single-stranded probe complementary to the *fraC* operon transcript (28), it might correspond to an antisense RNA. Indeed, the 1.35-kb transcript could be observed with a single-stranded probe identical to part of the *fraE* transcript (Fig. 1C, probe 2). This probe also hybridized to less-abundant RNA molecules of about 2.2 kb. These transcripts were regulated by the nitrogen source, being expressed at higher levels in nitrogen-fixing cultures than in cultures using ammonium or nitrate (Fig. 1B). Increased expression was also observed after N step-down (Fig. 1C, probe 2). Expression of these transcripts was impaired in strain CSE2 (*ntcA*) but not in strain 216 (*hetR*) (Fig. 1C, probe 2), indicating dependence on NtcA, which is consistent with N regulation, but not on HetR.

To test whether these antisense RNAs were extensions of the transcript of the downstream, oppositely oriented gene, *all2395* (Fig. 1A; see reference 44), Northern blot analysis with a probe of this gene (probe 4) and RNA isolated from filaments grown with ammonium or subjected to N depletion for several periods of time was performed. An inducible transcript of about 1.35 kb was evident, and a less-abundant RNA species of about 2.2 kb was also detected (Fig. 1D). The production of these transcripts was again largely dependent on the presence of NtcA but not on that of HetR. These results are consistent with the idea that the *fraE* antisense RNA corresponds to the *all2395* transcript.

The possible transcription start points (TSPs) for these RNAs were investigated by primer extension analysis using RNA isolated from filaments grown with ammonium and subjected (or not) to

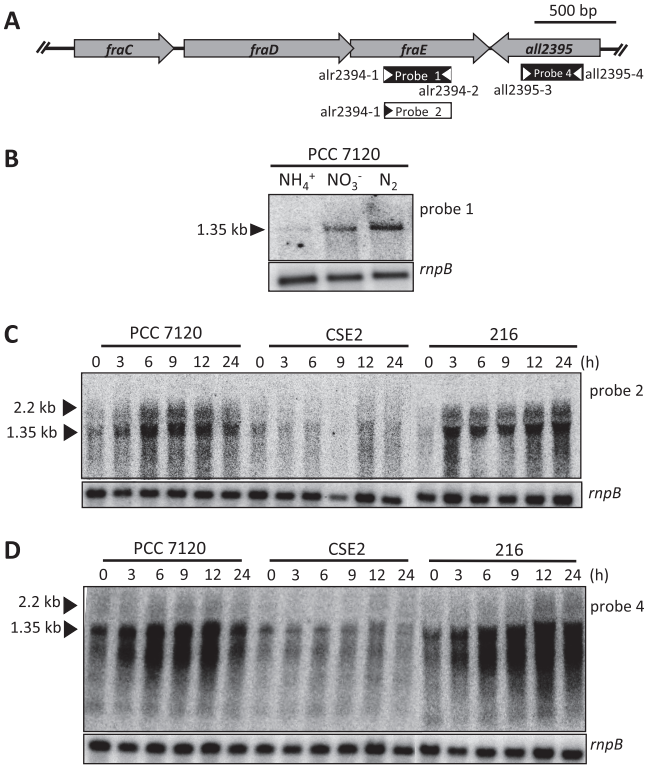

FIG 1 Northern blot analysis of the expression of *fraE* and α-*fraE*. (A) Scheme of the *fraC* operon region. Approximate locations of double-stranded (black) and single-stranded (white) probes are indicated. (B) Northern blot analysis performed with the indicated probe and RNA isolated from bubbled *Anabaena* cultures grown with ammonium, nitrate, or dinitrogen as the nitrogen source. (C and D) Northern blot analysis performed with the indicated probe and RNA isolated from bubbled cultures of strains PCC 7120 (wild type), CSE2 (*ntcA*), and 216 (*hetR*) grown with ammonium (0 h) and incubated without combined nitrogen for the number of hours indicated. Hybridization to a probe of the *rnpB* gene was used as a loading and transfer control for the different membranes. The sizes of some detected transcripts are indicated.

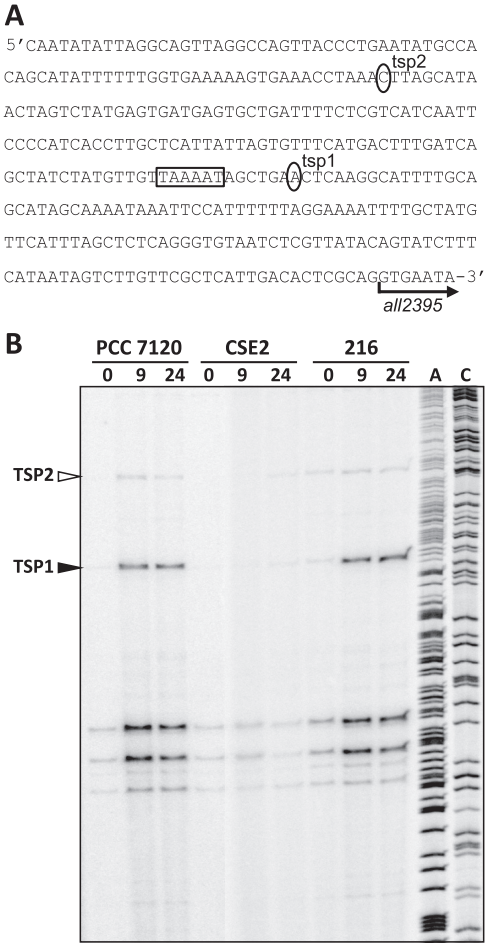

FIG 2 Primer extension analysis of the promoter region of *all2395*. (A) DNA sequence upstream of *all2395*. The start of the gene and the locations of putative TSPs and of a putative −10 promoter box (open box) are indicated. (B) Primer extension analysis carried out with primer all2395-9 and RNA from cultures of the indicated strains grown with ammonium and incubated without combined nitrogen for the indicated number of hours. "A" and "C" sequencing ladders are shown to the right.

N depletion for 9 or 24 h. Several RNA 5′ ends were detected that showed a regulation pattern similar to that of the 1.35- and 2.2-kb transcripts, including N regulation, dependence on the presence of NtcA, and independence of that of HetR (Fig. 2). One of these 5′ ends, which was located about 135 to 140 bp upstream of the start of the gene and is marked TSP1 in Fig. 2, was consistently observed with two different primers. This site is also found, positioned at 137 bp upstream of the start of the gene, in the recently published catalog of TSPs of *Anabaena* sp. strain PCC 7120 (45) and coincides with the start of a bulk of transcripts identified in a transcriptome analysis of this cyanobacterium (46). The strong bands found below TSP1 (Fig. 2B) could represent premature terminations in the primer extension reaction or extension on template degradation products. A putative −10 promoter hexamer (TAA AAT) is located upstream of TSP1 (Fig. 2), but no putative NtcA binding site (8) could be identified, suggesting that regulation by NtcA is indirect. Another possible transcription start point is located in the region around 285 bp upstream of the start of the gene (marked TSP2 in Fig. 2), but it was detected at a lower level than TSP1.

The distance between TSP1 and the end of *all2395* is 806 bp, whereas the distance to the start of *fraE* (*alr2304*) is 1,610 bp. These values indicate that the 1.35-kb *all2395* transcript can extend as an antisense RNA covering part of *fraE* whereas the 2.2-kb *all2395* transcript can extend to *fraD*, covering the whole *fraE* gene. To corroborate the presence of an antisense transcript covering *fraE*, RT-PCR was performed. Retrotranscription was carried out with RNA isolated from filaments incubated for 9 h in the absence of combined nitrogen and primers alr2393-7, alr2393-13, and alr2393-5 (Fig. 3A), and the respective reaction products were amplified by PCR with each of those primers and primer all2395-12 (Fig. 3A). PCR products were obtained with primer pair alr2393-13 and all2395-12 and primer pair alr2393-5 and all2395-12 but not with primer pair alr2393-7 and all2395-12 (Fig. 3B). These results are consistent with the presence of *all2395* transcripts of about 2.2 kb that reach *fraD* between primers alr2393-7 and alr2393-13. We collectively refer to the 1.35- and 2.2-kb transcripts as *all2395*-α-*fraE* here.

Construction of *all2395*-α-*fraE* mutants. Two *Anabaena* mutants affecting the *all2395*-α-*fraE* RNA were constructed as described in Materials and Methods. Mutant strain CSVT24 bears a

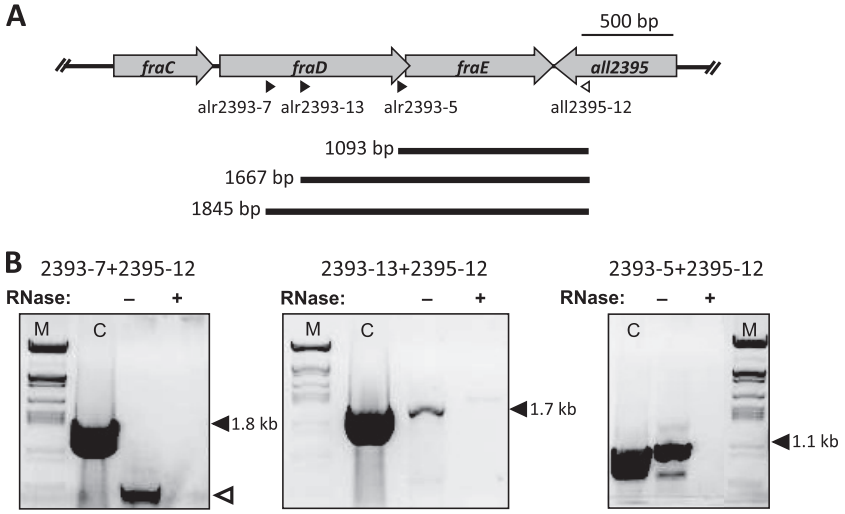

FIG 3 RT-PCR analysis of *all2395*-α-*fraE*. (A) Scheme of the *fraC* operon region, with indication of the primers used in the RT-PCR analysis and of the PCR products expected. (B) Results of the RT-PCR analysis carried out with RNA isolated from ammonium-grown bubbled cultures of wild-type strain PCC 7120 that were incubated under the same conditions for 9 h in the absence of combined nitrogen. Primers used for RT are indicated as black triangles in panel A. For PCR, each of those primers and primer all2395-12 (white triangle in panel A) were used. M, lambda DNA digested with ClaI; C, control PCR performed using genomic DNA as the template. The approximate size of the expected PCR product is indicated in each case. An unspecific product of about 550 bp (open arrowhead) is observed in the PCR with primer pair 2393-7 and 2395-12.

594-bp in-frame deletion of *all2395*, and mutant strain CSVT25 contains an insertion of gene cassette C.S3, which bears transcriptional terminators between *fraE* and *all2395* (Fig. 4A). Using a single-stranded probe complementary to the α-*fraE* transcript (probe 2 in Fig. 4A), an *all2395*-α-*fraE* transcript of about 0.67 kb was detected with RNA isolated from strain CSVT24 and no transcript was detected from strain CSVT25 (Fig. 4B), which is consistent with the genetic structure of these strains in the *fraE-all2395* region. Conversely, using a single-stranded probe complementary to the *all2395* transcript (probe 5 in Fig. 4A), no transcript was observed in strain CSVT24 and a transcript of about 0.82 kb was observed in strain CSVT25 (Fig. 4B).

The short transcripts observed in strains CSVT24 and CSVT25 with probes 2 and 5, respectively, showed N-dependent regulation similar to that seen with the whole *all2395*-α-*fraE* transcripts, but their cellular levels were altered compared to the wild-type transcripts (Fig. 4B). The levels of the 0.67-kb transcript of strain CSVT24 observed at 6 and 9 h after nitrogen deprivation were lower than the levels of the wild-type transcript (Fig. 4B, probe 2), and those of the 0.82-kb transcript of strain CSVT25 were higher than those of the wild-type transcript (Fig. 4B, probe 5). These results suggest that the introduced mutations affect the stability of the *all2395*-α-*fraE* transcripts.

Hybridization with a single-stranded probe complementary to *fraE* (probe 3 in Fig. 4A) detected RNA molecules of about 3.01 kb, which correspond to the operon transcript (28), in the wild type and in mutant CSVT24 (Fig. 4B) but a shorter transcript of about 2.4 kb in strain CSVT25. The distance from the putative TSP of *fraC* (located not farther than 117 bp upstream of the start codon [45]) to the end of *fraE* is 2,536 bp. These results indicate that the 3′ region of the *fraC* operon transcript also partially overlaps as an antisense RNA the downstream gene *all2395*. Q-RT-PCR analysis performed as described in Materials and Methods failed to show significant differences between the mutants and the wild type in the levels of the *fraC* operon transcript.

Phenotype of mutants producing altered *all2395*-α-*fraE*. Growth of the mutants was checked in liquid and solid medium. In liquid medium, both mutants grew at rates similar to that of the wild type in a manner independent of the nitrogen source (Table 2). In contrast, in solid medium, whereas growth of strain CSVT25 was little affected, growth of strain CSVT24 was clearly impaired specifically in the absence of combined nitrogen (Fig. 5).

In liquid cultures, mutant CSVT24 evidently formed clumps of filaments. Because diazotrophic cultures of the wild type also show some clumping, the effect of the mutation was most evident in cultures containing combined nitrogen (Fig. 6, top panel). Microscopic observation of these cultures confirmed the presence of clumps of filaments in strain CSVT24 whereas it showed a spread distribution of the filaments in the wild type and strain CSVT25 (Fig. 6). A closer look at the CSVT24 clumps showed the presence of fibers made of coiled filaments (Fig. 6). In these observations, it was also evident that strain CSVT24 produced particularly long filaments.

We determined filament lengths in cultures of the wild type and of mutants CSVT24 and CSVT25 grown with ammonium or grown with ammonium and incubated for 24 h in the absence of combined nitrogen, and the distributions of filament sizes in the mutants and the wild type were compared (Fig. 7). In strain CSVT24, long filaments were more numerous and short filaments were less numerous than in the wild-type strain both in the ammonium-grown cultures and after incubation without combined nitrogen. These results corroborated that strain CSVT24 exhibits increased filament length. In strain CSVT25, on the other hand, the filament size distribution was significantly different from the wild-type distribution only after nitrogen deprivation, when strain CSVT25 presented more long filaments and fewer short filaments than the wild type. However, long filaments were not as abundant in CSVT25 as in CSVT24 (Fig. 7). Interestingly, analysis of the distribution of filament sizes in the wild type showed that filaments were shorter after nitrogen deprivation than in the am-

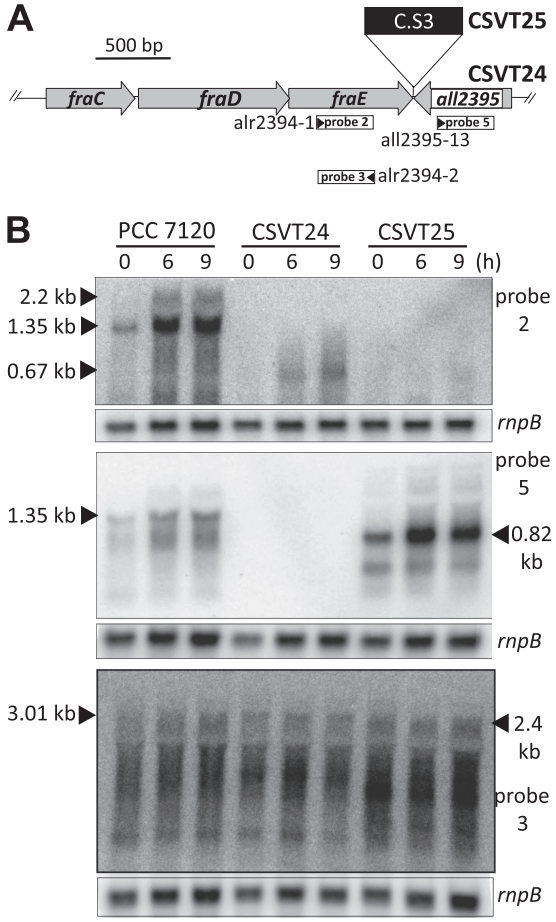

FIG 4 Northern blot analysis of the expression of the genes in the *fraC*-to-*all2395* gene cluster in mutant strains CSVT24 and CSVT25. (A) Scheme of the *fraC* operon region, with indication of the place of insertion of the C.S3 cassette and the location of the *all2395* deletion (white box). Approximate locations of single-stranded probes are also indicated. (B) Northern analysis carried out with the indicated probes and RNA from bubbled cultures of the indicated strains grown with ammonium and incubated for the indicated number of hours without combined nitrogen. Hybridization to a probe of the *rnpB* gene was used as a loading and transfer control for the different membranes. The sizes of some detected transcripts are indicated.

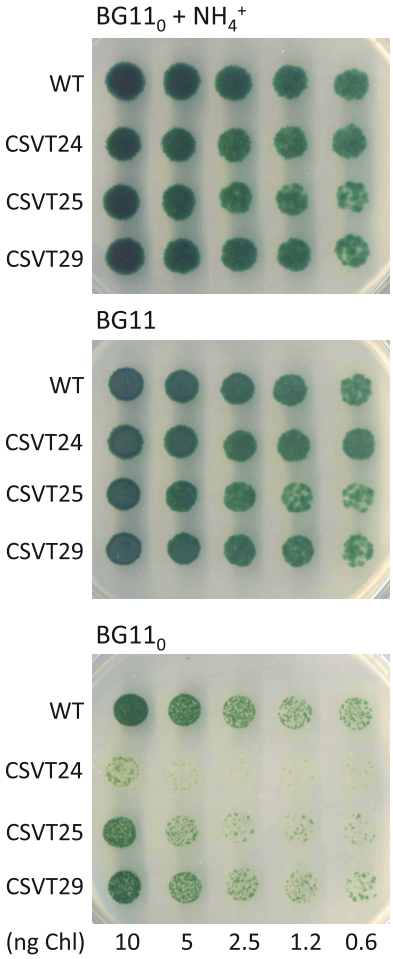

FIG 5 Growth of strains CSVT24, CSVT25, and CSVT29 on solid medium. Filaments of strains PCC 7120 (WT), CSVT24, CSVT25, and CSVT29 that had been grown with ammonium (in the presence of Sm and Sp for CSVT25) were harvested, washed with BG11$_0$ medium, and inoculated in solid medium containing ammonium (BG11$_0$ + NH$_4^+$) or nitrate (BG11) or without combined nitrogen (BG11$_0$). The different spots were inoculated with amounts of filaments containing the indicated amounts of Chl. The plates were incubated under culture conditions for 9 days and photographed.

monium-grown cultures ($P = 0.0036$). These observations indicate that the wild-type filaments experience some fragmentation after nitrogen step-down and that this fragmentation is restricted in the CSVT24 and CSVT25 mutants. Additionally, strain CSVT24, which lacks *all2395*, showed a long-filament phenotype also in media containing combined nitrogen in the form of either nitrate (Fig. 6) or ammonium (Fig. 7). We suggest that the protein product of *all2395* restricts filament length and denote this gene *fraF*.

TABLE 2 Growth rates of *Anabaena* sp. strain PCC 7120 and mutant strains in media containing the indicated nitrogen source[a]

Strain	Characteristic	Growth rate constant (μ, day^{-1})		
		NO_3^-	NH_4^+	N_2
PCC 7120	WT	0.790 ± 0.025	0.625 ± 0.070	0.565 ± 0.036
CSVT24	Internal deletion from *all2395*	0.851 ± 0.043	0.728 ± 0.023	0.592 ± 0.021
CSVT25	Insertion of C.S3 between *alr2394* and *all2395*	0.838 ± 0.075	0.709 ± 0.055	0.578 ± 0.008

[a] Cultures were inoculated at 0.2 μg Chl ml^{-1} using filaments grown with ammonium (in the presence of Sm and Sp for CSVT25) and washed with BG11$_0$ medium (lacking combined nitrogen). The cultures were incubated under culture conditions with the indicated nitrogen source.

Localization of expression of FraF. The place of expression of FraF in the filament was investigated using a translational GFP fusion. The gene encoding a superfolder GFP was added to the 3′ end of *fraF* (stop codon removed) with a joining oligonucleotide encoding a linker peptide (Fig. 8A). This construct was transferred to *Anabaena* sp. strain PCC 7120, producing strain CSVT29, which bears only chromosomes containing the altered fusion gene. Growth of strain CSVT29 on solid medium was more similar to that of the wild type than to that of mutant CSVT24 (Fig. 5), indicating that the fusion protein largely retains FraF function. Consistent with the results from Northern blot analysis, a low level of FraF-GFP fluorescence was observed in ammonium-grown filaments. After 24 h of incubation without combined nitrogen, increased fluorescence was observed, especially in heterocysts (Fig.

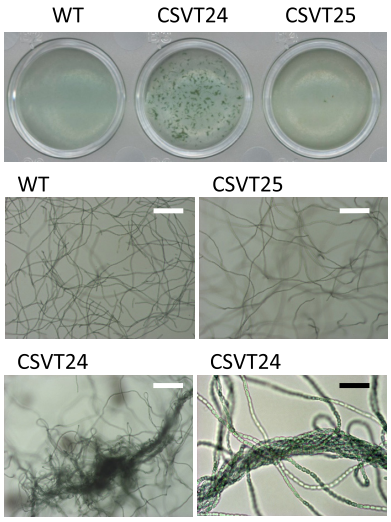

FIG 6 Filament clumping in strain CSVT24. Strains PCC 7120 (WT), CSVT24, and CSVT25 were grown in BG11 medium (in the presence of Sm and Sp for CSVT25) in a shaker. Samples from the corresponding cultures were transferred with great care to a microtiter plate, photographed (top panel), and used for microscopic inspection. Size markers: white bars, 100 μm; black bar, 10 μm.

8B). Quantification of the GFP fluorescence indicated a 2-to-2.5-fold-higher level in heterocysts than in vegetative cells (Fig. 8C). FraF-GFP appeared soluble in the cytoplasm, which is consistent with lack of a signal peptide in the FraF protein.

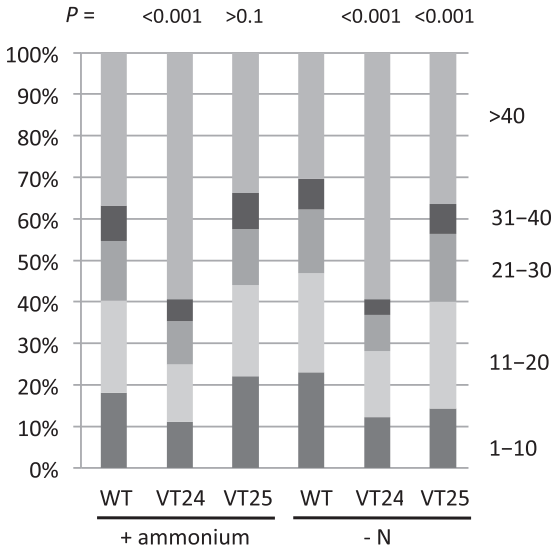

FIG 7 Distribution of filament lengths in *Anabaena* sp. strain PCC 7120 and strains CSVT24 and CSVT25. Samples of shaken cultures of strains PCC 7120 (WT), CSVT24 (VT24), and CSVT25 (VT25) grown with ammonium (in the presence of Sm and Sp for CSVT25) were taken with great care to avoid disruption of the filaments and counted (+ ammonium) or were washed with $BG11_0$ medium (lacking combined nitrogen) and incubated 24 h under the same culture conditions in $BG11_0$ medium, from which samples were taken with great care and counted (− N). A total of 550 filaments (from three independent experiments) corresponding to each strain and culture condition were ascribed to the indicated size intervals (size expressed as cells per filament, with grayscale code on the right; percentages of filaments are indicated on the left). For each growth condition, the distribution of filaments in each mutant was compared to that of the wild type using the χ^2 test (*P* indicated on top).

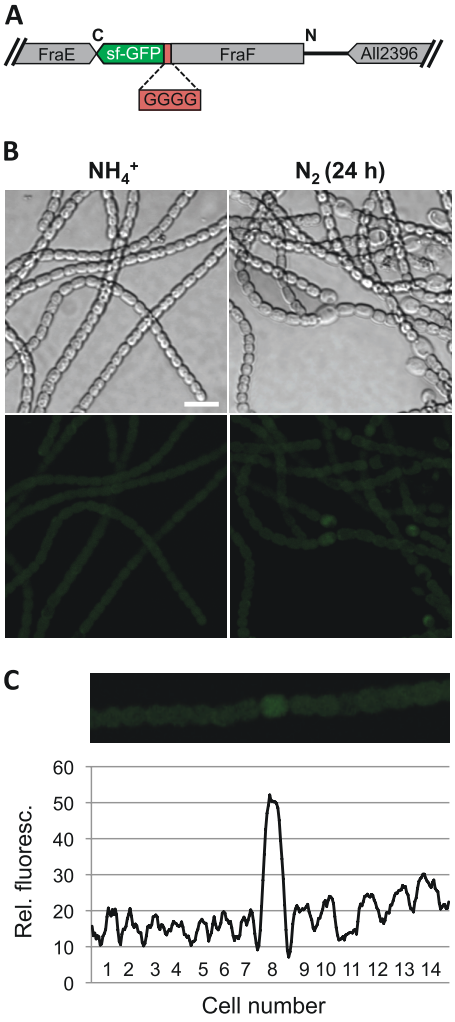

FIG 8 Localization of FraF expression. (A) Scheme of the FraF-GFP fusion that includes a tetrapeptide linker. (B) Samples of bubbled cultures of strain CSVT29 grown with ammonium or incubated for 24 h in medium lacking combined nitrogen were visualized by confocal microscopy. Bright-field (upper panels) and GFP fluorescence (lower panels) images are shown. (C) Quantification of GFP fluorescence from each cell along a filament of strain CSVT29. Average background fluorescence from wild-type cells (lacking the GFP) was subtracted. Cell no. 8 is a heterocyst. Rel. fluoresc., relative fluorescence.

DISCUSSION

In *Anabaena* sp. strain PCC 7120, the *fraC-fraD-fraE* operon is expressed in a transcript of about 3 kb that partly overlaps the downstream gene *fraF*, which lies tail to tail to *fraE*. Reciprocally, *fraF* transcripts of about 1.35 and 2.2 kb partially and totally overlap, respectively, the *fraE* gene, and the 2.2-kb transcript even reaches the *fraD* gene (Fig. 9). Disrupting these transcripts by introducing a gene cassette bearing transcriptional terminators between *fraE* and *fraF* (in strain CSVT25) results in increased levels of the *fraF* transcript (Fig. 4B, probe 5) but not of the *fraC* operon transcript. Upon incubation of the cultures in the absence of combined nitrogen, strain CSVT25 produces a higher frequency of long filaments and a lower frequency of short filaments than the wild type (Fig. 7). *cis* antisense RNAs can affect RNA stability and translation (18, 19). Although we do not know the

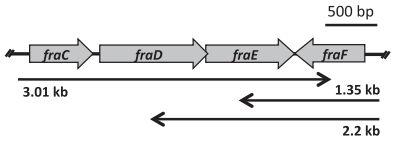

FIG 9 *cis* antisense RNAs in the *fra* gene cluster. The scheme shows the transcripts (horizontal arrows) that have been detected in the *fraC-fraD-fraE* ←*fraF* gene cluster. The TSP of the *fraC* operon has been assumed to be located not farther than 117 bp upstream from *fraC* (45). The *fraC* operon transcript is constitutive, whereas the *all2395*-α-*fraE* (*fraF*-α-*fraE*) transcripts are induced after nitrogen step down, leading to transcript levels that, at least for the 1.35-kb transcript, are higher than those of the *fraC* operon transcript (46).

precise mechanism(s), related to the presence of antisense RNAs, affecting the expression of genes in the *fraC-fraD-fraE*←*fraF* cluster (where the arrow indicates a change in orientation), increased translation of the *fraC* operon transcript in strain CSVT25 might be considered.

Deletion of *fraF* (in strain CSVT24) produced a significant increase in the frequency of long filaments in both the presence and the absence of combined nitrogen (Fig. 7). Long, coiled filaments formed structures seen as fibers (Fig. 6). We do not know whether these structures could result simply from a lack of filament breakage. Strain CSVT24 additionally shows impaired growth specifically in solid medium. These phenotypic alterations of strain CSVT24 could result from an increased translation of the *fraC* operon transcript (related to the decreased levels of α-*fraE* transcript observed in this strain; Fig. 4, probe 2) or from a lack of FraF. However, because longer filaments were observed in strain CSVT24, which produces α-*fraE* transcript, than in strain CSVT25, which produces no α-*fraE* transcript, and because growth was more affected in strain CSVT24 than in strain CSVT25 (Fig. 5), the FraF protein appears to be important to limit filament length and to optimize diazotrophic growth on solid medium.

In contrast to the *fraC* operon, which appears to be constitutive (28), *fraF* is induced under conditions of nitrogen deprivation (see also reference 46) in a way that is dependent on NtcA but not on HetR (Fig. 1D; see also reference 45). Interestingly, however, analysis of expression of a FraF-GFP fusion shows induction mainly in heterocysts (Fig. 8). Although deletion of *fraF* produces a phenotypic alteration in the presence of combined nitrogen (Fig. 6 and 7), dependence of *fraF* expression on the presence of NtcA is consistent with the fact that growth impairment of the Δ*fraF* mutant is most evident under diazotrophic conditions, under which NtcA is most active (7, 8). Thus, expression of *fraF* is increased under conditions of nitrogen deprivation, producing a protein, FraF, which is needed to keep the *Anabaena* filaments at an appropriate length for proper diazotrophic growth on a surface. The role of FraF may be especially relevant for the fragmentation of filaments that takes place after N step-down, but why the length of the filaments must be limited is unknown. Few studies have addressed the role of filament length in the physiology of cyanobacteria (see, e.g., reference 47), and few studies have addressed whether mechanisms exist that regulate filament length. It has been suggested that trichome breakage in the heterocyst-forming cyanobacterium *Calothrix elenkinii* is a mechanism allowing the fragmented filaments to escape from unfavorable environmental conditions (48). Although *Anabaena* sp. strain PCC 7120 has been described as nonmotile (31), it would be interesting to know whether gliding motility, which is frequent among filamentous cyanobacteria (31, 49), is influenced by filament length.

Analysis of the FraF amino acid sequence shows that it is a pentapeptide repeat protein, one of a family of proteins containing a repeated five-residue domain (50). FraF is homologous to other pentapeptide repeat proteins, such as HglK (51), HetL (52), and PatL (53), that are involved in heterocyst differentiation. Whereas the pentapeptide repeat domain in HglK or PatL is only a part of a protein that contains other large domains, the pentapeptide repeat domain in HetL and FraF constitutes most of the protein. The crystal structure of several pentapeptide repeat proteins, including HetL, has been determined (see reference 54 and references therein). These proteins adopt a highly regular four-sided right-handed ß helical structure. A prediction of the structure of FraF performed with the Phyre server (55) renders a structure very similar to that of HetL. In other bacteria, pentapeptide repeat proteins can be found in different cellular compartments, and reported functions range from inhibition of DNA gyrase (56) to regulation of manganese uptake (50). We cannot currently envisage a mechanism of action for FraF, but its genomic location might imply a relation to the positive filamentation proteins encoded in the *fraC* operon. FraF could interfere with the function of other Fra proteins, which might be most relevant at the junctions between differentiating heterocysts and vegetative cells. Interestingly, the filaments of an *Anabaena ntcA* mutant overexpressing HetL are highly fragmented (52), which might establish a connection between the functions of FraF and HetL. HetL stimulates heterocyst differentiation, but a *hetL* null mutant is not impaired in diazotrophic growth, perhaps because of redundancy with other pentapeptide repeat proteins (52).

In summary, our results show that *Anabaena* sp. strain PCC 7120 bears a gene, *fraF*, that negatively affects filament length and is needed for optimal growth under certain conditions (i.e., diazotrophic growth on a surface). Thus, *fraC-fraD-fraE*←*fraF* appears to constitute a gene cluster involved in determining the morphology of this cyanobacterium. Among the products of this gene cluster, FraF has an effect that is opposite to that of FraC, FraD, and FraE, which are needed for *Anabaena* sp. to make long filaments mainly in the absence of combined nitrogen. Additionally, overlap of the *fraC* operon and *fraF* gene transcripts (Fig. 9), with the *fraF* transcript being expressed at higher levels than the *fraC* operon transcript under conditions of nitrogen deprivation (46), could affect production of the corresponding proteins. Some *cis*-acting antisense RNAs produced in clusters of divergent genes that are somehow related in function have been described, leading to the definition of the "excludon" as a paradigm in RNA-mediated gene regulation (19). Here we have presented an example of *cis* antisense RNAs produced between convergent genes of related function but having opposite effects. This arrangement may represent an excellent way to fine-tune the regulation of genes with opposite roles.

The coverage of sequenced cyanobacterial genomes has recently been improved (57, 58), which allows performing informed studies on the distribution of particular genes in the cyanobacteria. As analyzed in the U.S. Department of Energy Joint Genome Institute (DOE JGI) Genome Portal (http://img.jgi.doe.gov/cgi-bin/w/main.cgi), the *fraC* operon is widely conserved in filamentous cyanobacteria, and it is present in all the sequenced genomes of heterocyst-forming cyanobacteria. Among these, the *fraC-fraD-fraE*←*fraF* gene cluster is found in about 60% (14 of 23) of the genomes. In two additional genomes, the cluster is present but contains one or more genes between the *fraC* operon and *fraF*. The

frequent conservation of the *fraC-fraD-fraE←fraF* gene arrangement in a significant number of heterocyst-forming cyanobacteria suggests that the function of restricting filament length, complementary to the filamentation function of the proteins encoded in the *fraC* operon, enhances the fitness of those heterocyst-forming cyanobacteria.

ACKNOWLEDGMENTS

We thank A. López-Lozano, V. Mariscal, and M. Burnat (Instituto de Bioquímica Vegetal y Fotosíntesis, Sevilla, Spain) for providing plasmid pCSAL34, for quantification of GFP fluorescence, and for some growth tests, respectively. We also thank Josep Casadesús (Departamento de Genética, Universidad de Sevilla) for facilitating the Q-RT-PCR analysis.

This work was supported by grants BFU2008-03811 and BFU2011-22762 from the Spanish government, cofinanced by FEDER.

REFERENCES

1. **Flärdh K, Buttner MJ.** 2009. *Streptomyces* morphogenetics: dissecting differentiation in a filamentous bacterium. Nat. Rev. Microbiol. **7:**36–49.
2. **Pierson BK, Castenholz RW.** 1974. A phototrophic gliding filamentous bacterium of hot springs, Chloroflexus aurantiacus, gen. and sp. nov. Arch. Microbiol. **100:**5–24.
3. **Pfeffer C, Larsen S, Song J, Dong M, Besenbacher F, Meyer RL, Kjeldsen KU, Schreiber L, Gorby YA, El-Naggar MY, Leung KM, Schramm A, Risgaard-Petersen N, Nielsen LP.** 2012. Filamentous bacteria transport electrons over centimetre distances. Nature **491:**218–221.
4. **Flores E, Herrero A.** 2010. Compartmentalized function through cell differentiation in filamentous cyanobacteria. Nat. Rev. Microbiol. **8:**39–50.
5. **Kumar K, Mella-Herrera RA, Golden JW.** 2010. Cyanobacterial heterocysts. Cold Spring Harb. Perspect. Biol. **2:**a000315.
6. **Xu X, Elhai J, Wolk CP.** 2008. Transcriptional and developmental responses by *Anabaena* to deprivation of fixed nitrogen, p 383–422. *In* Herrero A, Flores E (ed), The cyanobacteria. Molecular biology, genomics and evolution. Caister Academic Press, Norfolk, United Kingdom.
7. **Herrero A, Picossi S, Flores E.** 2013. Gene expression during heterocyst differentiation. Adv. Bot. Res. **65:**281–329.
8. **Herrero A, Muro-Pastor AM, Flores E.** 2001. Nitrogen control in cyanobacteria. J. Bacteriol. **183:**411–425.
9. **Vázquez-Bermúdez MF, Flores E, Herrero A.** 2002. Analysis of binding sites for the nitrogen-control transcription factor NtcA in the promoters of *Synechococcus* nitrogen-regulated genes. Biochim. Biophys. Acta **1578:** 95–98.
10. **Sutcliffe IC.** 2010. A phylum level perspective on bacterial cell envelope architecture. Trends Microbiol. **18:**464–470.
11. **Hoiczyk E, Hansel A.** 2000. Cyanobacterial cell walls: news from an unusual prokaryotic envelope. J. Bacteriol. **182:**1191–1199.
12. **Flores E, Herrero A, Wolk CP, Maldener I.** 2006. Is the periplasm continuous in filamentous multicellular cyanobacteria? Trends Microbiol. **14:**439–443.
13. **Mariscal V, Herrero A, Flores E.** 2007. Continuous periplasm in a filamentous, heterocyst-forming cyanobacterium. Mol. Microbiol. **65:**1139–1145.
14. **Schneider D, Fuhrmann E, Scholz I, Hess WR, Graumann PL.** 2007. Fluorescence staining of live cyanobacterial cells suggest non-stringent chromosome segregation and absence of a connection between cytoplasmic and thylakoid membranes. BMC Cell Biol. **8:**39.
15. **Wilk L, Strauss M, Rudolf M, Nicolaisen K, Flores E, Kühlbrandt W, Schleiff E.** 2011. Outer membrane continuity and septosome formation between vegetative cells in the filaments of *Anabaena* sp. PCC 7120. Cell. Microbiol. **13:**1744–1754.
16. **Waters LS, Storz G.** 2009. Regulatory RNAs in bacteria. Cell **136:**615–628.
17. **Storz G, Vogel J, Wassarman KM.** 2011. Regulation by small RNAs in bacteria: expanding frontiers. Mol. Cell **43:**880–891.
18. **Georg J, Hess WR.** 2011. *cis*-antisense RNA, another level of gene regulation in bacteria. Microbiol. Mol. Biol. Rev. **75:**286–300.
19. **Sesto N, Wurtzel O, Archambaud C, Sorek R, Cossart P.** 2013. The excludon: a new concept in bacterial antisense RNA-mediated gene regulation. Nat. Rev. Microbiol. **11:**75–82.
20. **Georg J, Voss B, Scholz I, Mitschke J, Wilde A, Hess WR.** 2009. Evidence for a major role of antisense RNAs in cyanobacterial gene regulation. Mol. Syst. Biol. **5:**305.
21. **Backofen R, Hess WR.** 2010. Computational prediction of sRNAs and their targets in bacteria. RNA Biol. **7:**33–42.
22. **Hernández JA, Muro-Pastor AM, Flores E, Bes MT, Peleato ML, Fillat MF.** 2006. Identification of a *furA cis* antisense RNA in the cyanobacterium *Anabaena* sp. PCC 7120. J. Mol. Biol. **355:**325–334.
23. **Buikema WJ, Haselkorn R.** 1991. Isolation and complementation of nitrogen fixation mutants of the cyanobacterium *Anabaena* sp. strain PCC 7120. J. Bacteriol. **173:**1879–1885.
24. **Ernst A, Black T, Cai Y, Panoff JM, Tiwari DN, Wolk CP.** 1992. Synthesis of nitrogenase in mutants of the cyanobacterium *Anabaena* sp. strain PCC 7120 affected in heterocyst development or metabolism. J. Bacteriol. **174:**6025–6032.
25. **Bauer CC, Buikema WJ, Black K, Haselkorn R.** 1995. A short-filament mutant of *Anabaena* sp. strain PCC 7120 that fragments in nitrogen-deficient medium. J. Bacteriol. **177:**1520–1526.
26. **Nayar AS, Yamaura H, Rajagopalan R, Risser DD, Callahan SM.** 2007. FraG is necessary for filament integrity and heterocyst maturation in the cyanobacterium *Anabaena* sp. strain PCC 7120. Microbiology **153:**601–603.
27. **Flores E, Pernil R, Muro-Pastor AM, Mariscal V, Maldener I, Lechno-Yossef S, Fan Q, Wolk CP, Herrero A.** 2007. Septum-localized protein required for filament integrity and diazotrophy in the heterocyst-forming cyanobacterium *Anabaena* sp. strain PCC 7120. J. Bacteriol. **189:**3884–3890.
28. **Merino-Puerto V, Mariscal V, Mullineaux CW, Herrero A, Flores E.** 2010. Fra proteins influencing filament integrity, diazotrophy and localization of septal protein SepJ in the heterocyst-forming cyanobacterium *Anabaena* sp. Mol. Microbiol. **75:**1159–1170.
29. **Mariscal V, Herrero A, Nenninger A, Mullineaux CW, Flores E.** 2011. Functional dissection of the three-domain SepJ protein joining the cells in cyanobacterial trichomes. Mol. Microbiol. **79:**1077–1088.
30. **Merino-Puerto V, Schwarz H, Maldener I, Mariscal V, Mullineaux CW, Herrero A, Flores E.** 2011. FraC/FraD-dependent intercellular molecular exchange in the filaments of a heterocyst-forming cyanobacterium, Anabaena sp. Mol. Microbiol. **82:**87–98.
31. **Rippka R, Deruelles J, Waterbury JB, Herdman M, Stanier RY.** 1979. Generic assignments, strain histories and properties of pure cultures of cyanobacteria. J. Gen. Microbiol. **111:**1–61.
32. **Ausubel FM, Brent R, Kingston RE, Moore D, Seidman JG, Smith JA, Struhl K.** 2012. Current protocols in molecular biology. Greene Publishing and Wiley-Interscience, New York, NY.
33. **Cai YP, Wolk CP.** 1990. Use of a conditionally lethal gene in *Anabaena* sp. strain PCC 7120 to select for double recombinants and to entrap insertion sequences. J. Bacteriol. **172:**3138–3145.
34. **Valladares A, Rodríguez V, Camargo S, Martínez-Noël GMA, Herrero A, Luque I.** 2011. Specific role of the cyanobacterial PipX factor in the heterocysts of *Anabaena* sp. strain PCC 7120. J. Bacteriol. **193:**1172–1182.
35. **Black TA, Cai Y, Wolk CP.** 1993. Spatial expression and autoregulation of *hetR*, a gene involved in the control of heterocyst development in *Anabaena*. Mol. Microbiol. **9:**77–84. (Erratum,**10:**1153.)
36. **Elhai J, Wolk CP.** 1988. A versatile class of positive-selection vectors based on the nonviability of palindrome-containing plasmids that allows cloning into long polylinkers. Gene **68:**119–138.
37. **Elhai J, Vepritskiy A, Muro-Pastor AM, Flores E, Wolk CP.** 1997. Reduction of conjugal transfer efficiency by three restriction activities of *Anabaena* sp. strain PCC 7120. J. Bacteriol. **179:**1998–2005.
38. **Paz-Yepes J, Herrero A, Flores E.** 2007. The NtcA-regulated *amtB* gene is necessary for full methylammonium uptake activity in the cyanobacterium *Synechococcus elongatus*. J. Bacteriol. **189:**7791–7798.
39. **Vioque A.** 1997. The RNase P RNA from cyanobacteria: short tandemly repeated repetitive (STRR) sequences are present within the RNase P RNA gene in heterocyst-forming cyanobacteria. Nucleic Acids Res. **25:**3471–3477.
40. **Muro-Pastor AM, Valladares A, Flores E, Herrero A.** 1999. The *hetC* gene is a direct target of the NtcA transcriptional regulator in cyanobacterial heterocyst development. J. Bacteriol. **181:**6664–6669.
41. **Montesinos ML, Herrero A, Flores E.** 1995. Amino acid transport systems required for diazotrophic growth in the cyanobacterium *Anabaena* sp. strain PCC 7120. J. Bacteriol. **177:**3150–3157.
42. **Markwell MAK, Hass SM, Bieber LL, Tolbert NE.** 1978. A modification

of the Lowry procedure to simplify protein determination in membrane and lipoprotein samples. Anal. Biochem. **87:**206–210.
43. **Mackinney G.** 1941. Absorption of light by chlorophyll solutions. J. Biol. Chem. **140:**109–112.
44. **Kaneko T, Nakamura Y, Wolk CP, Kuritz T, Sasamoto S, Watanabe A, Iriguchi M, Ishikawa A, Kawashima K, Kimura T, Kishida Y, Kohara M, Matsumoto M, Matsuno A, Muraki A, Nakazaki N, Shimpo S, Sugimoto M, Takazawa M, Yamada M, Yasuda M, Tabata S.** 2001. Complete genomic sequence of the filamentous nitrogen-fixing cyanobacterium *Anabaena* sp. strain PCC 7120. DNA Res. **8:**205–213.
45. **Mitschke J, Vioque A, Haas F, Hess WR, Muro-Pastor AM.** 2011. Dynamics of transcriptional start site selection during nitrogen stress-induced cell differentiation in *Anabaena* sp. PCC7120. Proc. Natl. Acad. Sci. U. S. A. **108:**20130–20135.
46. **Flaherty BL, van Nieuwerburgh F, Head SR, Golden JW.** 2011. Directional RNA deep sequencing sheds new light on the transcriptional response of *Anabaena* sp. strain PCC 7120 to combined-nitrogen deprivation. BMC Genomics **12:**332.
47. **Tamulonis C, Postma M, Kaandorp J.** 2011. Modeling filamentous cyanobacteria reveals the advantages of long and fast trichomes for optimizing light exposure. PLoS One **6:**e22084.
48. **Adamec F, Kaftan D, Nedbal L.** 2005. Stress-induced filament fragmentation of *Calothrix elenkinii* (Cyanobacteria) is facilitated by death of high-fluorescence cells. J. Phycol. **41:**835–839.
49. **Hoiczyk E.** 2000. Gliding motility in cyanobacteria: observations and possible explanations. Arch. Microbiol. **174:**11–17.
50. **Chandler LE, Bartsevich VV, Pakrasi HB.** 2003. Regulation of manganese uptake in *Synechocystis* 6803 by RfrA, a member of a novel family of proteins containing a repeated five-residues domain. Biochemistry **42:**5508–5514.
51. **Black K, Buikema WJ, Haselkorn R.** 1995. The hglK gene is required for localization of heterocyst-specific glycolipids in the cyanobacterium *Anabaena* sp. strain PCC 7120. J. Bacteriol. **177:**6440–6448.
52. **Liu D, Golden JW.** 2002. HetL overexpression stimulates heterocyst formation in *Anabaena* sp. strain PCC 7120. J. Bacteriol. **184:**6873–6881.
53. **Liu J, Wolk CP.** 2011. Genes *patA* and *patL* of *Anabaena* sp. strain PCC 7120 have similar mutant phenotypes, and their products may interact. J. Bacteriol. **193:**6070–6074.
54. **Ni S, Sheldrick GM, Benning MM, Kennedy MA.** 2009. The 2Å resolution crystal structure of HetL, a pentapeptide repeat protein involved in regulation of heterocyst differentiation in the cyanobacterium *Nostoc* sp. strain PCC 7120. J. Struct. Biol. **165:**47–52.
55. **Kelley LA, Sternberg MJE.** 2009. Protein structure prediction on the Web: a case study using the Phyre server. Nat. Protoc. **4:**363–371.
56. **Hegde SS, Vetting MW, Roderick SL, Mitchenall LA, Maxwell A, Takiff HE, Blanchard JS.** 2005. A fluoroquinolone resistance protein from *Mycobacterium* tuberculosis that mimics DNA. Science **308:**1480–1483.
57. **Dagan T, Roettger M, Stucken K, Landan G, Koch R, Major P, Gould SB, Goremykin VV, Rippka R, Tandeau de Marsac N, Gugger M, Lockhart PJ, Allen JF, Brune I, Maus I, Pühler A, Martin WF.** 2013. Genomes of stigonematalean cyanobacteria (subsection V) and the evolution of oxygenic photosynthesis from prokaryotes to plastids. Genome Biol. Evol. **5:**31–44.
58. **Shih PM, Wu D, Latifi A, Axen SD, Fewer DP, Talla E, Calteau A, Cai F, Tandeau de Marsac N, Rippka R, Herdman M, Sivonen K, Coursin T, Laurent T, Goodwin L, Nolan M, Davenport KW, Han CS, Rubin EM, Eisen JA, Woyke T, Gugger M, Kerfeld CA.** 2013. Improving the coverage of the cyanobacterial phylum using diversity-driven genome sequencing. Proc. Natl. Acad. Sci. U. S. A. **110:**1053–1058.